The fluid sloshing in a vertical circular cylindrical tank with a rigid-ring baffle I: Linear fundamental solutions*

I. Gavrilyuk[1], I. Lukovsky[2], Yu. Trotsenko[2] and A. Timokha[3†]

[1] *Berufakademie Thüringen-Staatliche Studienakademie, Am Wartenberg 2, 99817, Eisenach, Germany;*
[2] *Institute of Mathematics, National Academy of Sciences of Ukraine, Tereschenkivska 3, 01601 Kiev, Ukraine;*
[3] *Friedrich-Schiller-Universität Jena, Institut für Angewandte Mathematik, Ernst-Abbe-Platz 2-4, Jena, 07745, Germany*

Abstract

The paper centres around fundamental solutions of a linear evolutional problem which describes fluid sloshing in a vertical circular cylindrical tank with a thin rigid-ring horizontal baffle fitted to the inner walls. Under certain postulations accepted for those hydrodynamic systems, the paper adopts inviscid fluid model with irrotational flows and, thereupon, places emphasis on quantifying natural frequencies and modes versus both position and width of the baffle. The analysis is based on an analytically-oriented variational method which gives accurate approximate solutions capturing asymptotic behaviour of the velocity potential at the sharp baffle edge. Forthcoming Part II will use the analytical approximate solutions in a nonlinear modal modelling and in computing the damping due to local vorticity stress.

Keywords: *Linear Fluid Sloshing, Natural Frequencies, Rigid Baffle, Galerkin's Method, Transmission*

MSC (1991): 35R35, 76B07

Introduction

A fluid occupying partly either earth-fixed or moving tanks of rockets, nuclear reactors, tower- and bridge constructions, ships and liquefied natural gas carriers performs wave motions, the sloshing, that are caused by time-dependent and instantaneous perturbations of its hydrostatic equilibrium. Since the fluid sloshing disturbed by guidance and control systems commands, ship manoeuvres and structural vibrations of mobile vessels generates significant hydrodynamic force- and moment loads on the moving tank, it becomes a danger for structural integrity and can produce a dramatical feedback sensed and responded by to the tank motions forming a closed loop that leads to an instability, tank bulkheads and even damage. In view of minimising the crucial loads, preventing structural failure and governing the fluid position within the tank, extensive experimental and theoretical studies have been undertaken from several decades ago and, as a result, numerous devices have

*The work is partially supported by Deutsche Forschungsgemeinschaft.

†The author acknowledges sponsorship by the Alexander von Humboldt Foundation and the Centre for Ship and Ocean Structures, NTNU, Norway

been designed for suppressing the fluid mobility. These devices use fact that the structural instability hazard is explainable by the closeness of a control structural frequency to a fundamental sloshing frequency. This closeness yields, over and above the gust inputs, coupled resonant vibrations involving large sloshing mass and, as a consequence, leading to non-controllability and even destruction of the whole object. In order to diminish the fluid effects to structural stability, the lowest fundamental sloshing frequencies should be shifted away from the control frequency domain. Systematic analysis of the passive devices which influence the natural sloshing frequencies has at different time and for different applications been given by Abramson [1], Bauer [5], Mikishev & Rabinovich [38], Mikishev & Churilov [37], Mikishev [36] and Ibrahim *et al.* [28]. Design criteria by Abramson [1] give a series of suitable engineering solutions consisting for instance of subdividing the container by longitudinal (vertical) walls (Bauer [3, 4]). However, the compartment is characterised by increasing structural mass and the baffling is in many cases the cheaper method without the weight penalty.

While engineering of mobile vehicles with fluids requires the splitting of structural and sloshing frequency domains, the so-called tuned sloshing dampers of large buildings, towers and bridges suggests their overlapping. This makes it possible to redistribute the total kinetic energy of the whole object in behalf of the fluid mass and, since the fluid motions have in many cases larger damping rates than the rigid/elastic structures, to increase the resulting dissipation with consequent mitigation of structural vibrations. In that case, the theoretical analysis becomes more complicated, because it should be based on fully nonlinear formulation. This implies requirements in robust and accurate computer programs (see reviews by Solaas [48], Moan & Berge [41] and Cariou & Casella [9] and some successful simulations of the baffled fluid sloshing by Arai *et al.* [2], Campolo *et al.* [8], Celebi & Akyildiz [10] and Cho & Lee [13, 14]).

Physical nature of the tuner sloshing dampers is found quite different for distinct tanks' shapes and fluid fillings. As explained by Ockendon *et al.* [44], Faltinsen & Timokha [21] and Yalla [53]), the tuned sloshing dampers with small fluid depths employ features of shallow fluid flows. The fundamental sloshing spectrum of the shallow fluid layer is nearly-commensurate and, therefore, nonlinearity leads in this case to progressive resonant activation of higher modes which are responsible for short, steep surface waves. Since these short wave phenomena are accompanied by local breaking and dramatically effected by viscosity and surface tension, the kinetic sloshing energy dissipates very rapidly and desirable structural damping can be achieved even without slosh-suppressing devices. In contrast, the sloshing in smooth tanks with a finite fluid depth resembles to the long free-standing waves which, if baffles are not introduced, have small damping rates (see, reviews on its quantification by Yalla [53], Faltinsen & Timokha [20], Faltinsen *et al.* [19]). An explanation of the physical nature of the tuned sloshing dampers is based on changing the steady-state nonlinear resonant response (see two-dimensional numerical results by Ikeda & Nakagawa [29] and Cho & Lee [14]) and the damping due to vorticity forces at the sharp baffle edges. The latter has been in primary focus of many investigations including Keulegan & Carpenter [31], Miles [39], Silveira *et al.* [47], Mikishev & Rabinovich [38], Mikishev [36], Sarpkaya & O'Keefe [46]), and, recently, Isaacson & Premasiri [30] and Buzhinskii [7]. They showed that, if the surface wave magnitude is relatively small, the vorticity-based logarithmic decrements can be quantified in the framework of linear hydrodynamic theory based on inviscid potential model. The analysis introduces the so-called velocity intensity factor, the coefficient K_v appearing at the main singular term of the linear velocity potential along the sharp baffle edge. By mentioning that an analogous problem arises in linear fracture mechanics (when calculating the stress intensity factors on the sharp edges of cracks in a solid) Buzhinskii [7] discusses difficulties to quantify K_v in sloshing problems by traditional Computational Fluid Mechanics (CFD) methods. He calls for analytically-oriented approaches that capture singular behaviour of the fundamental linear solution.

The need in analytically-oriented approaches to fluid sloshing in tanks with baffles has motivated us to undertake a special applied mathematical studies. We restricted ourselves to the case of relatively simple tank geometry, exemplified in this paper by a vertical circular cylinder. The research project pursued three consequent, linked goals: (i) the development of analytically-oriented methods for the linearised fluid sloshing problem that approximate the natural spectrum of the free-standing wave modes as precise as the singular asymptotics of the linear fundamental solutions at the baffle edge; (ii) the generalisation of nonlinear modal methods for theoretical classification of steady-state resonant fluid motions in similar manner as it has been done by Lukovsky [35], Faltinsen *et al.* [19, 18] and Gavrilyuk *et al.* [24] for smooth cylindrical tanks; (iii) an analytical quantification of the fluid damping due to vorticity stress at the baffle edge by utilising both Buzhinskii's formula [7]. The problem on analytical approximations of the linear fundamental solutions, the core of the project, is investigated in the present paper.

The linear fluid sloshing in a circular cylindrical tank with rigid baffles has been studied by many authors in context of spacecraft applications. Experimental and numerical results are reported by Dokuchaev [15], Bauer [5], Rabinovich [45], Ermakov *et al.* [17], Trotsenko [49], Morozov [43] and, recently, by Watson & Evans [52], Biswal *et al.* [6] and Gedikli & Ergüven [26, 27]. Since the task of these papers consists basically in quantifying the lower natural sloshing frequency, almost all theoretical and numerical investigation were based on classical finite element schemes that provide sufficient accuracy in computing the primary natural tone. To the authors knowledge, there is very limited set of numerical approaches which take into account analytical features of the velocity potential at the baffle edge. Three of the rare examples are represented in papers by Galitsin & Trotsenko [23], Trotsenko [50] and Gavrilyuk *et al.* [25] devoted to two-dimensional linear sloshing in a rectangular tank with two horizontal baffles. After detailed reading these papers, we found it possible to develop similar method in more general cases including the tanks of circular base. As a result, we obtained a very efficient and precise semi-analytical solver which gives six significant figures of the fundamental frequencies with small (up to 8) number of the basis functions. Abilities of the method are demonstrated by numerical examples. The analysis of fundamental sloshing spectrum versus geometric size of the baffle and its position has also been done. The failure of the method is detected when either baffle is very close to the mean fluid surface or baffle is sufficiently wide to prevent fluid current between lower (under the baffle) and upper (over the baffle) fluid domains. We give mathematical and physical treatment of these failures as well as note that decreasing length between the baffle plate and the hydrostatic fluid surface leads in practise to either the baffle stripping or the shallow wave motions over the baffle.

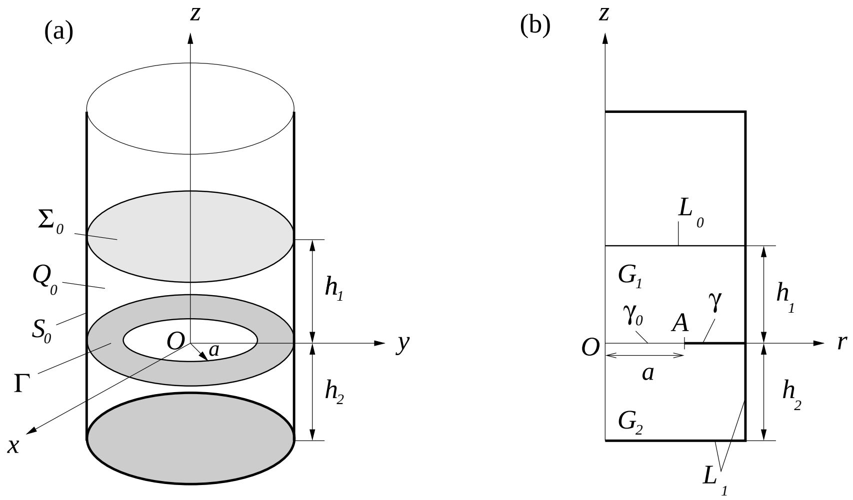

Fig. 1. Hydrostatic fluid shape in a rigid cylindrical tank; three-dimensional and meridional sketches. The thin rigid-ring baffle Γ is submerged into the fluid volume.

1. Statement of the problem

1.1. Theory

Let a rigid circular base cylindrical tank of the radius R be partially filled by a fluid with the mean depth h. The inner periphery of the tank contains a thin rigid ring-plate baffle which divides the amount fluid height h into h_1 and h_2, where h_1 is the mean height of fluid layer over the baffle and h_2 is the length between the baffle and the bottom. The thickness of the baffle is assumed to be negligible relative to h_1 and h_2. The fluid motions occurring due to initial perturbations are furthermore described in the framework of the inviscid incompressible hydrodynamic model with irrotational flows. In order to conserve the baffle inside of the fluid bulk (the sloshing does not strip the baffle), the free-standing waves deflections relative to hydrostatic plane are assumed to be smaller than h_1.

The problem is studied in the size-dimensionless formulation suggesting that all lengths and physical constants are normalised by the circular base radius R. This implies in particular that $h_1 := h_1/R, h_2 := h_2/R, g := g/L_1$ (the gravity acceleration g has now the dimension $[s^{-2}]$) etc. The free boundary problem is formulated in the tank-fixed coordinate system $Oxyz$. The Oz-axis is directed along the symmetry axis of the tank and the origin O is posed in the plane of the baffle as shown for hydrostatic case in Figure 1 (a). Further, we assume small initial perturbations that initialise the linear free-standing gravity waves. Under certain circumstances, these waves can be found from the following problem (Feschenko *et al.* [22])

$$\Delta\tilde{\Phi} = 0 \ \text{ in } Q_0; \quad \frac{\partial\tilde{\Phi}}{\partial\nu} = 0 \ \text{ on } S_0 \text{ and } \Gamma; \quad \int_{\Sigma_0} \frac{\partial\tilde{\Phi}}{\partial z} dS = 0, \tag{1.1a}$$

$$\frac{\partial\tilde{\Phi}}{\partial z} = \frac{\partial\tilde{f}}{\partial t}; \qquad \frac{\partial\tilde{\Phi}}{\partial t} + g\tilde{f} = 0 \ \text{ on } \Sigma_0, \tag{1.1b}$$

where Q_0 is the static fluid domain, S_0 is the statically wetted tank surface, Σ_0 coincides with the mean fluid surface, $\boldsymbol{\nu}$ is the outward normal to Q_0, the function $\tilde{f}(x,y,t)$ defines small-amplitude deviations of the free surface evolution ($z = \tilde{f}(x,y,t)$) and $\tilde{\Phi}(x,y,z,t)$ denotes the linear velocity potential. The boundary value problem (1.1) should be accomplished by the initial conditions

$$\tilde{f}(0,x,y) = \tilde{f}_0(x,y); \quad \frac{\partial \tilde{f}}{\partial t}(0,x,y) = \tilde{f}_1(x,y), \quad \int_{\Sigma_0} \tilde{f}_i dS = 0, \ i = 1,2, \tag{1.2}$$

where the prescribed small-norm functions $\tilde{f}_0$ and $\tilde{f}_1$ define initial deviations and velocities of the free surface, respectively.

Solutions of the linear problem (1.1) are associated with a special class of spectral problems with spectral parameter in boundary conditions. This suggests the substitution

$$\tilde{\Phi}(x,y,z,t) = \varphi(x,y,z) \ \exp(I\omega t), \ I^2 = -1, \tag{1.3}$$

which introduces the natural frequency ω and the natural mode $\varphi(x,y,z)$. By rewriting the boundary conditions (1.1b) to the form

$$\frac{\partial^2 \tilde{\Phi}}{\partial t^2} + g\frac{\partial \tilde{\Phi}}{\partial z} = 0; \quad \tilde{f} = -\frac{1}{g}\frac{\partial \tilde{\Phi}}{\partial t} \quad \text{on } \Sigma_0 \tag{1.4}$$

and introducing $\kappa = \omega^2/g$, the evolutional problem (1.1a) (1.4) is transformed to

$$\begin{aligned} &\Delta\varphi = 0 \quad \text{in } Q_0; \quad \frac{\partial \varphi}{\partial \nu} = 0 \quad \text{on } S_0 \text{ and } \Gamma, \\ &\frac{\partial \varphi}{\partial z} = \kappa\varphi \quad \text{on } \Sigma_0; \quad \int_{\Sigma_0} \varphi dS = 0. \end{aligned} \tag{1.5}$$

As established by Eastham [16], the spectral problem (1.5) has a real positive pointer spectrum $\{\kappa_i\}$, $\kappa_i \to +\infty$ and $\{\varphi_i(x,y,0)\}$ put together an orthogonal basis in $L_2(\Sigma_0)$ for any functions which satisfy the last integral condition of (1.5). These spectral theorems deduce that eigenfunctions of (1.5) constitute, via formula (1.3), the fundamental solution of the evolutional problem (1.1): Having known $\tilde{f}_0$ and $\tilde{f}_1$ in (1.2) we can find $\tilde{\Phi}$ by using the Fourier series in $\{\varphi_i(x,y,z)\}$, the natural frequencies are determined by $\omega_i = \sqrt{g\kappa_i}$.

1.2. Natural modes in a circular-base tank with a ring baffle

When Q_0 has axial-symmetric shape, the spectral problem (1.5) allows for separation of spatial variables in the (r,η,z)-cylindrical coordinate system, e.g. $x = r\cos\eta, y = r\sin\eta, z = z$. Introducing $\varphi^{(m)}(r,\eta,z) = \psi^{(m)}(z,r)\exp(Im\eta)$, $m = 0,1,\ldots$ reduces (1.5) to the m-parametric family of the two-dimensional spectral problems in the meridional cross-section of Q_0:

$$\begin{aligned} &L_m(\psi^{(m)}) = \frac{\partial^2 \psi^{(m)}}{\partial r^2} + \frac{1}{r}\frac{\partial \psi^{(m)}}{\partial r} + \frac{\partial^2 \psi^{(m)}}{\partial z^2} - m^2\psi^{(m)} = 0 \quad \text{in } G, \\ &\frac{\partial \psi^{(m)}}{\partial r} = 0 \quad \text{on } L_1; \quad \frac{\partial \psi^{(m)}}{\partial z} = 0 \quad \text{on } \gamma; \quad \psi^{(m)}(z,0) < \infty, \\ &\frac{\partial \psi^{(m)}}{\partial z} = \kappa^{(m)}\psi^{(m)} \quad \text{on } L_0, \quad m = 0,1,\ldots; \quad \int_{L_0} r\psi^{(0)} dr = 0, \end{aligned} \tag{1.6}$$

where geometric definitions of G, L_1, L_0 and γ are sketched in Figure 1 (b).

Simple analysis shows that (1.6) has an analytical solution for either $a = 1$ (there is not baffle) or $a = 0$ (the horizontal baffle completely splits the tank into two non-connected volumes). Explicit expressions for the natural spectra $\kappa[h]_i^{(m)}$ and $\kappa[h_1]_i^{(m)}$, $i \geq 1$ (eigenvalues are posed in ascending order with i) can be written down as

$$\kappa[h]_i^{(m)} = \alpha_{i,m}\tanh(\alpha_{i,m}h); \quad \kappa[h_1]_i^{(m)} = \alpha_{i,m}\tanh(\alpha_{i,m}h_1), \tag{1.7}$$

where $\alpha_{i,m}$ is the ith root of the equation $J'_m(\alpha_{i,m}) = 0$ ($J_m(x)$ is the Bessel function of first kind). The eigenfunctions take the form

$$\begin{aligned} \varphi[h]_i^{(m)} &= J_m(\alpha_{i,m}r)\frac{\cosh(\alpha_{i,m}(z+h_2))}{\cosh(\alpha_{i,m}h)}\begin{cases}\cos n\eta,\\ \sin m\eta,\end{cases} \\ \varphi[h_1]_i^{(m)} &= J_m(\alpha_{i,m}r)\frac{\cosh(\alpha_{i,m}(z))}{\cosh(\alpha_{i,m}h_1)}\begin{cases}\cos n\eta,\\ \sin m\eta.\end{cases} \end{aligned} \tag{1.8}$$

Spectral theorems given by Feschenko *et al.* [22] and Lukovsky *et al.* [34] show that eigenvalues of (1.6) lay between $\kappa[h_1]_i^{(m)}$ and $\kappa[h]_i^{(m)}$, i.e.

$$\kappa[h_1]_i^{(m)} \leq \kappa_i^{(m)} \leq \kappa[h_1]_i^{(m)}, \quad i = 1, 2, \ldots; \quad m = 0, 1, \ldots. \tag{1.9}$$

2. Approximate fundamental solutions

2.1. Variational method

If $0 < a < 1$, the spectral problems (1.6) have not analytical solutions. Following Galitsin & Trotsenko [23] and Trotsenko [50], let us consider an artificial $\gamma_0 = \{z = 0,\ 0 \leqslant r < a\}$ that cuts (together with $\gamma = \{z = 0,\ a \leqslant r \leqslant 1\}$) the original meridional domain G into two rectangles G_1 and G_2 as shown in Figure 1 (b). The original solution $\psi^{(m)}$ falls then into two functions defined in G_1 and G_2 as follows

$$\psi^{(m)}(z,r) = \begin{cases}\psi^{(m,1)}(z,r), & (z,r) \in G_1,\\ \psi^{(m,2)}(z,r), & (z,r) \in G_2.\end{cases} \tag{2.1}$$

These function must satisfy

$$L_m(\psi^{(m,i)}) = 0 \ \text{ in } G_i, \quad \psi^{(m,i)}(z,0) < \infty, \quad i = 1, 2, \tag{2.2}$$

and the boundary conditions following from (1.6), i.e.

$$\begin{aligned} &\frac{\partial \psi^{(m,1)}}{\partial r} = 0 \ \ (r = 1,\ 0 < z < h_1); \quad \frac{\partial \psi^{(m,1)}}{\partial z} = 0 \ \ (z = 0,\ a < r < 1), \\ &\frac{\partial \psi^{(m,1)}}{\partial z} = \kappa^{(m)}\psi^{(m,1)} \ \ (z = h_1,\ 0 < r < 1); \end{aligned} \tag{2.3}$$

for $\psi^{(m,1)}$, and

$$\frac{\partial\psi^{(m,2)}}{\partial r}=0 \quad (r=1,\ -h_2<z<0);\quad \frac{\partial\psi^{(m,2)}}{\partial z}=0 \quad (z=0,\ a<r<1),$$
$$\frac{\partial\psi^{(m,2)}}{\partial z}=0 \quad (z=-h_2,\ 0<r<1). \tag{2.4}$$

for $\psi^{(m,2)}$.

In addition, since the original $\psi^{(m)}(r,z)$ and their first derivatives should be continuous at γ_0, (2.2)-(2.4) must be accomplished on γ_0 by the following transmission conditions

$$\psi^{(m,1)}(r,0)=\psi^{(m,2)}(r,0) \quad (0<r<a), \tag{2.5a}$$

$$\frac{\partial\psi^{(m,1)}}{\partial z}=\frac{\partial\psi^{(m,2)}}{\partial z}=N_m^{(\kappa^{(m)})}(r) \quad (0<r<a), \tag{2.5b}$$

where $N_m^{(\kappa^{(m)})}(r)$ is an auxiliary function from $L_2(0,a)$ depending on $\kappa^{(m)}$. Besides, when $m=0$, the integral condition of (1.6) leads to

$$\int_{L_0} r\psi^{(0,1)}dr=0 \quad \text{and} \quad \int_0^a rN_0^{\kappa^{(m)}}(r)dr=0.$$

Further, we consider a transmission procedure, which inputs the test spectral parameter $\kappa^{(m)}\notin\{\kappa_i^{(m)}[h_1],\ i=1,2,\ldots\}$ and assumes that the test function $N_m^{\kappa^{(m)}}(r)$ is known. By combining (2.3)–(2.5b) we get two boundary value problems (2.2)+(2.3)+(2.5b) and (2.2)+(2.4)+(2.5b), which have the analytical Green functions

$$K_m^{(\kappa^{(m)})}(r,z;r_0,z_0)=\sum_{k=1}^{\infty}\frac{J_m(\alpha_{km}r)J_m(\alpha_{km}r_0)}{\alpha_{km}n_{km}^2\sinh(\alpha_{km}h_1-\vartheta_{km})}\cosh[\alpha_{km}(z-h_1)+$$
$$+\vartheta_{km}]\cosh(\alpha_{km}z_0), \quad ((r,z),(r_0,z_0)\in G_1; z>z_0), \tag{2.6a}$$

$$K_m(r,z;r_0,z_0)=\sum_{k=1}^{\infty}\frac{J_m(\alpha_{km}r)J_m(\alpha_{km}r_0)}{\alpha_{km}n_{km}^2\sinh(\alpha_{km}h_2)}\cosh[\alpha_{km}(z+h_2)]\cosh(\alpha_{km}z_0),$$
$$((r,z),(r_0,z_0)\in G_2; z>z_0), \tag{2.6b}$$

where

$$\vartheta_{km}=\ln\left|\frac{\alpha_{km}+\kappa^{(m)}}{\alpha_{km}-\kappa^{(m)}}\right|;\ n_{km}^2=\int_0^1 rJ_m^2(\alpha_{km}r)dr=\frac{1}{2}\left(1-\frac{m^2}{\alpha_{km}^2}\right)J_m^2(\alpha_{km}).$$

These Green functions compute

$$\psi^{(m,1)}(z,r)=-\int_0^a N_m^{\kappa^{(m)}}(r)K_m^{(\kappa^{(m)})}(z,r;0,r_0)r_0dr_0,$$
$$\psi^{(m,2)}(z,r)=\int_0^a N_m^{\kappa^{(m)}}(r)K_m(z,r;0,r_0)r_0dr_0+\delta_{0m}\text{const} \tag{2.7}$$

(δ_{im} is the Kronecker delta).

The solutions (2.7) must satisfy the transmission condition (2.5a), which leads to the integral equation

$$\int_0^a \left[K_m(h_1,r,0,r_0)+K_m^{(\kappa^{(m)})}(h_1,r;0,r_0)\right]N_m^{\kappa^{(m)}}(r)r_0dr_0=\delta_{0m} \tag{2.8}$$

with respect to $N_m^{\kappa^{(m)}}$ and $\kappa^{(m)}$. A way to solve this integral equation consists of the Galerkin variational method. This implies the series

$$N_m^{\kappa^{(m)}}(r)=\sum_{p=1}^{\infty}X_p^{(m,\kappa^{(m)})}f_p^{(m)}(r)\quad(0<r<a), \tag{2.9}$$

where $\{X_p^{(m,\kappa^{(m)})}\}$ are unknown and $\{f_p^{(m)}\}$ is a two-parametric family of the $L_2(0,a)$-complete functions (the case $m=0$ requires $\int_0^a rf_p^{(0)}(r)dr=0,\ p=1,2,\ldots$). The integral equation (2.8) can be reduced to the two-parametric equalities

$$\int_0^a\left(\psi^{(m,1)}(r,0)-\psi^{(m,2)}(r,0)\right)rf_q^{(m)}(r)dr=0,\quad p,q=1,2,\ldots, \tag{2.10}$$

or, more precisely, to the following infinite-dimensional system of linear homogeneous algebraic equations with respect to $X_p^{(m,\kappa^{(m)})}$

$$\lim_{p_0\to\infty}\sum_{p=1}^{p_0}X_p^{(m,\kappa^{(m)})}A_{pq}^{(\kappa^{(m)},m)}=0,\quad(q=1,2,3,\ldots), \tag{2.11}$$

where

$$\begin{aligned}A_{pq}^{(\kappa^{(m)},m)}&=\sum_{k=1}^{\infty}B_{pk}^{(m)}B_{qk}^{(m)}\alpha_{km}n_{km}^2\left[\coth(\alpha_{km}h_2)+\frac{\kappa^{(m)}\tanh(\alpha_{km}h_1)-\alpha_{km}}{\kappa^{(m)}-\alpha_{km}\tanh(\alpha_{km}h_1)}\right],\\ B_{pk}^{(m)}&=\frac{1}{\alpha_{km}n_{km}^2}\int_0^a f_p^{(m)}(r)J_m(\alpha_{km}r)rdr.\end{aligned} \tag{2.12}$$

The linear system (2.11) has non-trivial solution, if and only if, the test value $\kappa^{(m)}$ coincides with an eigenvalue from (1.6). When truncating (2.11), the necessary solvability condition

$$\det\|\ \{A_{pq}^{(\kappa^{(m)},m)},\ p,q=1,\ldots,p_0\}\ \|=0 \tag{2.13}$$

can be considered as a transcendental equation with respect to the test numbers $\kappa^{(m)}$. Therefore, the roots of (2.13) output the approximate eigenvalues $\{\kappa_p^{(m)},\ p=1,2,\ldots,p_0\}$ as well as enable calculation of approximate eigenfunctions. The latter suggests the usage of non-trivial solutions $\{X_p^{(m,n)}\}$ of (2.11) and the integral presentation (see, Watson [51])

$$J_{\mu+\nu+1}(z)=\frac{z^{\nu+1}}{2^{\nu}\Gamma(\nu+1)}\int_0^{\frac{\pi}{2}}J_\mu(z\sin\vartheta)\sin^{\mu+1}\vartheta\cos^{2\nu+1}\vartheta d\vartheta,$$

with the gamma-function $\Gamma(x)$, which deduces

$$\begin{aligned} \psi_n^{(m,1)}(z,r) &= -\sum_{k=1}^{\infty} a_k^{(m,n)} J_m(\alpha_k r) g_k^{(m,n)}(r), \\ \psi_n^{(m,2)}(z,r) &= \sum_{k=1}^{\infty} a_k^{(m,n)} J_m(\alpha_k r) g_k^{(m)}(r), \quad (m = 0,1,2,\ldots), \end{aligned} \tag{2.14}$$

where

$$\begin{aligned} a_k^{(m,n)} &= \sum_{p=1}^{\infty} X_p^{(m,\kappa_n^{(m)})} b_{pk}^{(m)}, \quad b_{pk}^{(m)} = \widetilde{b}_{pk}^{(m)} - \delta_{0m}\frac{2p+1}{2p-1}\widetilde{b}_{p+1,k}^{(m)}, \\ \widetilde{b}_{pk}^{(m)} &= \frac{a^{m+2} 2^{p-\frac{3}{2}} \Gamma\left(p-\frac{1}{2}\right) J_{m+p-\frac{1}{2}}(\alpha_{km} a)}{\alpha_{km} n_{km}^2 (\alpha_{km} a)^{p-\frac{1}{2}}}, \\ g_k^{(m,n)} &= \frac{\cosh[\alpha_{km}(z-h_1)]}{\cosh(\alpha_{km} h_1)} \cdot \frac{\alpha_{km} + \kappa_n^{(m)} \tanh[\alpha_{km}(z-h_1)]}{\alpha_{km}\tanh(\alpha_{km} h_1) - \kappa_n^{(m)}}, \\ g_k^{(m)} &= \frac{\cosh[\alpha_{km}(z+h_2)]}{\sinh(\alpha_{km} h_2)}. \end{aligned}$$

2.2. Functional basis

Accuracy, convergence and numerical effectiveness of the variational method depend on the functional basis $\{f_p^{(m)}\}$ used in (2.9). Since

$$\frac{\partial \psi^{(m)}}{\partial z} \sim \sqrt{\frac{a}{2\pi}} \frac{1}{\sqrt{1-(\frac{r}{a})^2}} \ \text{as } r \to a; \quad \frac{\partial \psi^{(m)}}{\partial z} \sim r^m, \ \text{as } r \to 0 \tag{2.15}$$

(Lukovsky *et al.*[34]), the basis has to have special asymptotic behaviour at $r = 0$ and a, respectively.

A simplest example of such basis that is used in the present paper reads

$$\begin{aligned} f_p^{(m)}(r) &= \frac{r^m}{\sqrt{1-\left(\frac{r}{a}\right)^2}} \left[1-\left(\frac{r}{a}\right)^2\right]^{p-1}, \quad (m,p = 1,2,\ldots), \\ f_p^{(0)}(r) &= f_p^{(*)}(r) - \frac{2p+1}{2p-1} f_{p+1}^{(*)}(r) \quad (m=0; p=1,2,\ldots), \end{aligned} \tag{2.16}$$

where

$$f_p^{(*)}(r) = \left[1-\left(\frac{r}{a}\right)^2\right]^{p-\frac{3}{2}}.$$

Remark 2.1. Since $A_{pq}^{(\kappa^{(m)},m)}$, $p,q = 1,\ldots,p_0$ are determined by the series (2.12) which are functions of $\kappa^{(m)}$, accuracy in computing roots of the transcendental equation (2.13) will depend on convergence of (2.12). By using

$$\alpha_{km} \approx k\pi; \quad J_m^2(\alpha_{km}) \approx \frac{2}{\pi^2 k}, \quad k \to \infty, \tag{2.17}$$

one can show that elements of (2.12) are

$$O\left(\frac{1}{k^{p+q}}\right), \quad m = 0, 1, 2, \dots; \; p, q = 1, 2, \dots \tag{2.18}$$

and, therefore, the case $p = q = 1$ is characterised by weak convergence. In order to improve this convergence, one can account for (2.17) and take in mind that the series

$$S_m = \frac{2a^{2m+2}}{\pi} \sum_{k=1}^{\infty} \frac{\phi_k^{(m)}}{k^2}, \quad \phi_k^{(m)} = \begin{cases} \sin^2 k\pi a, & (m = 0, 2), \\ \cos^2 k\pi a, & (m = 1) \end{cases}$$

are computed analytically with the following result

$$S_m = \begin{cases} \pi a^{2m+3}(1 - a), & (m = 0, 2), \\ \pi a^4 \left(\frac{1}{3} + a^2 - a\right), & (m = 1). \end{cases}$$

This makes it possible to re-write (2.12) for $p = q = 1$ to the following form

$$\alpha_{11}^{(\kappa,m)} = S_m + \\ + \sum_{k=1}^{\infty} \left\{ (b_{1k}^{(m)})^2 \alpha_{km} n_{km}^2 [\coth(\alpha_{km} h_2) + \coth(\alpha_{km} h_1 - \vartheta_k^{(m,n)})] - \frac{2a^{2m+2} \varphi_k^{(m)}}{k^2 \pi} \right\},$$

where the modified numerical series has the asymptotics $O(k^{-3})$ instead of $O(k^{-2})$.

3. Numerical results

3.1. Convergence

When using the functional basis (2.16), the proposed Galerkin method shows good convergence for different values of h_1, h_2 and a. This can be viewed in Table 1 representing $\kappa_i^{(m)}$, $i = 1, 2, 3, 4$ $(m = 0, 1, 2)$ versus p_0. If $h_1 \geq 0.1$ and $a \geq 0.3$, the numerical method guarantees six significant figures of $\kappa_1^{(m)}$ $(m = 0, 1, 2)$ with the truncation size $p_0 = 5$. Approximation of some of higher eigenvalues need $p_0 = 8$ to get the same accuracy.

One should note, that calculations of approximate $\kappa^{(m)}$ from the transcendental equations (2.13) are usually based on an iterative methods and, therefore, the effectiveness and stability of our algorithm may depend on initial approximations. We tested various solvers of the transcendental equations. When $h_1 \geq 0.1$ and $a \geq 0.3$, all of them provide stable computing with arbitrary initial $\kappa^{(m)}$ from the range determined by inequalities (1.9). The situation changed for lower h_1 and a, when the solvers became unstable and a special care of initial approximation has been needed. Typical way that has been used in our numerical

Table 1. Convergence of $\kappa_n^{(0)}, \kappa_n^{(1)}$ and $\kappa_n^{(2)}$, $n = 1, 2, 3, 4$ versus truncation size p_0 in (2.13) for $a = 0.7$, $h_2 = 0.5$ and two values of $h_1 = 0.1$ and 0.5.

		$h_1 = 0.1$			$h_1 = 0.5$		
n	p_0	$\kappa_n^{(0)}$	$\kappa_n^{(1)}$	$\kappa_n^{(2)}$	$\kappa_n^{(0)}$	$\kappa_n^{(1)}$	$\kappa_n^{(2)}$
1	1	2.28607	0.93790	1.53476	3.75597	1.62183	2.90455
	2	2.28653	0.94024	1.53544	3.75910	1.62404	2.90621
	3	2.28654	0.94027	1.53544	3.75912	1.62404	2.90621
	4	2.28655	0.94028	1.53544	3.75912	1.62404	2.90621
	5	2.28655	0.94028	1.53544	3.75912	1.62404	2.90621
	6	2.28655	0.94028	1.53544	3.75912	1.62404	2.90621
	7	2.28655	0.94028	1.53544	3.75912	1.62404	2.90621
2	1	4.81039	2.98097	4.68493	7.00504	5.28665	6.69385
	2	6.12230	4.15960	5.88364	7.01042	5.31058	6.70035
	3	6.19683	4.18504	5.93413	7.01088	5.31187	6.70077
	4	6.19733	4.18506	5.93441	7.01089	5.31188	6.70078
	5	6.19734	4.18506	5.93441	7.01089	5.31188	6.70078
	6	6.19734	4.18506	5.93441	7.01089	5.31188	6.70078
	7	6.19734	4.18506	5.93441	7.01089	5.31188	6.70078
3	1	8.29360	6.26769	8.02229	10.17280	8.53331	9.96865
	2	8.55123	6.66552	8.39313	10.17294	8.53395	9.96887
	3	9.50380	7.82773	9.31368	10.17322	8.53525	9.96919
	4	9.60561	7.92096	9.39597	10.17326	8.53539	9.96923
	5	9.60785	7.92226	9.39760	10.17326	8.53539	9.96923
	6	9.60788	7.92227	9.39761	10.17326	8.53539	9.96923
	7	9.60788	7.92227	9.39761	10.17326	8.53539	9.96923
4	1	11.60040	9.68234	11.40933	13.32365	11.70581	13.17032
	2	11.86938	10.04555	11.66641	13.32365	11.70584	13.17033
	3	12.09188	10.29531	11.94871	13.32366	11.70588	13.17034
	4	12.70927	11.05345	12.56100	13.32368	11.70594	13.17035
	5	12.80440	11.14807	12.64583	13.32368	11.70595	13.17036
	6	12.80820	11.15087	12.64899	13.32368	11.70595	13.17036
	7	12.80827	11.15091	12.64905	13.32368	11.70595	13.17036

tests consisted in implementing a path-following procedure with respect to the two real parameters h_1 and a. The procedure computed the roots of (2.13) for the fixed $h_1 < 0.1$ and $a < 0.3$ with initial $\kappa^{(m)}$ obtained as roots of (2.13) for larger h_1 and a. This path-following made it possible to extend the results for $h_1 > 0.01$ and $a > 0.1$. However, it showed sensitivity to stepping in h_1 and a, especially for the dimensions $p_0 \geq 5$, and failed for $h_1 \leq 0.01$ and $a \leq 0.1$.

Numerical failure for $h_1 \to 0$. While good convergence of our variational method for non-small h_1 is caused by adequate functional basis which captures the actual asymptotic behaviour of $N_m^{\kappa^{(m)}} = \partial\psi^{(m)}/\partial z(r, 0)$ at $r = a$ and 0, its numerical failure for smaller h_1 needs special studies. Mathematically, it can be explained by the fact that the spectral problem (1.6) with $h_1 = 0$ (the baffle lies on the unperturbed free surface), which describes the fluid sloshing in a circular hole, has other, logarithmic asymptotics for $\partial\psi^{(m)}/\partial z$ at $r = a$, which is inconsistent with our functional basis. Detailed mathematical analysis of the corresponding spectral problem is given by Kozlov *et al.* [32] and Kuznetsov & Motygin [33].

An alternative, physical treatment of the numerical failure involves a shallow fluid analysis of the fluid layer over the rigid plate assuming that $h_1/(1-a) \to 0$. By using prediction of the shallow-like sloshing $h_1/(1-a) \lesssim 0.2$ given by Faltinsen & Timokha [21], we deduce strongly nonlinear and dissipative surface waves (Chester [11] and Chester & Bones [12]) which are not described by our inviscid linear fluid model for $h_1 < 0.1$ and $a < 0.3$. This means that any results based on linear inviscid model for small h_1 can be irrelevant.

Numerical failure for $a \to 0$. Even if h_1 is not small, our method can be invalid for small a, namely, when the baffle is relatively wide to prevent fluid flows between the upper and lower fluid domains. This numerical failure is caused by using the Green technique in our variational method. If a thin rigid-ring baffle is fitted in the inner fluid periphery, the eigenvalues $\kappa_i^{(m)}$ are not only confined to (1.9), but also depend monotonically on a. Theoretically, by using the spectral theorem documented by Feschenko *et al.* [22] we deduce that when the baffle is introduced further and further into the fluid, the spectral values $\kappa_i^{(m)}$, $m = 0, 1, \ldots; i = 1, 2, \ldots$ change from its corresponding value in the absence of the baffle to the natural frequencies than it corresponding to the two separate fluids, i.e.

$$\kappa_i^{(m)} \to \kappa[h_1]_i^{(m)} + 0 \ \text{ as } a \to 0 \ \text{ and } \ \kappa_i^{(m)} \to \kappa[h]_i^{(m)} - 0 \ \text{ as } a \to 1. \tag{3.1}$$

Accounting for the first limit we can see that if a test value $\kappa^{(m)}$ approximates solution with small a, it is close to one from $\kappa[h_1]_i^{(m)}$, $i = 1, 2, ...$, and therefore the Green function (2.6a) becomes degenerate. The reason is the ill-possedness of the boundary value problem (2.2)+(2.3)+(2.5b) and consequent division by zero in (2.6a), when at least one root of (2.13) tends to an isolated $\kappa[h_1]_i^{(m)}$. On the other hand, the failure for $a \to 0$ implies that fundamental solutions are close to those without baffle, and the latter can be used in practical calculations.

The limitations on h_1 and a restricted our systematical study of the linear baffled sloshing to the domain $0.1 \le h_1$ and $0.3 < a$, where the Galerkin scheme is stable and guarantees high accuracy.

3.2. Natural surface wave profiles

By using the second boundary condition of (1.4) the linear fundamental solutions $\varphi_j(x, y, z)$, $j \ge 1$, determine standing wave profiles (natural surface modes) as follows

$$z = F_j(r, \eta) = \kappa_j \varphi_j(r, \eta, 0) = \frac{\partial \varphi_j}{\partial z}(r, \eta, 0), \quad j \ge 1. \tag{3.2}$$

Splitting angular (in terms η) and radial (along r) components and noting that the angular steepness is defined by the trigonometric functions, we focus furthermore on the two-dimensional projections in the meridional cross-section

$$z = F_i^{(m)}(r) = \kappa_i^{(m)} \psi_i^{(m)}(r, 0), \quad m = 0, 1, \ldots;\ i = 1, 2, \ldots. \tag{3.3}$$

Our analytically-oriented method is applicable to compute $F_i^{(m)}(r)$. Some examples of the radial profiles are drawn in Figure 2. These examples leave traces the curves $z = F_i^{(m)}$, $m = 0, 1, 2$; $i = 1, 2, 3$ versus a. The figures show that, as it has been predicted, if

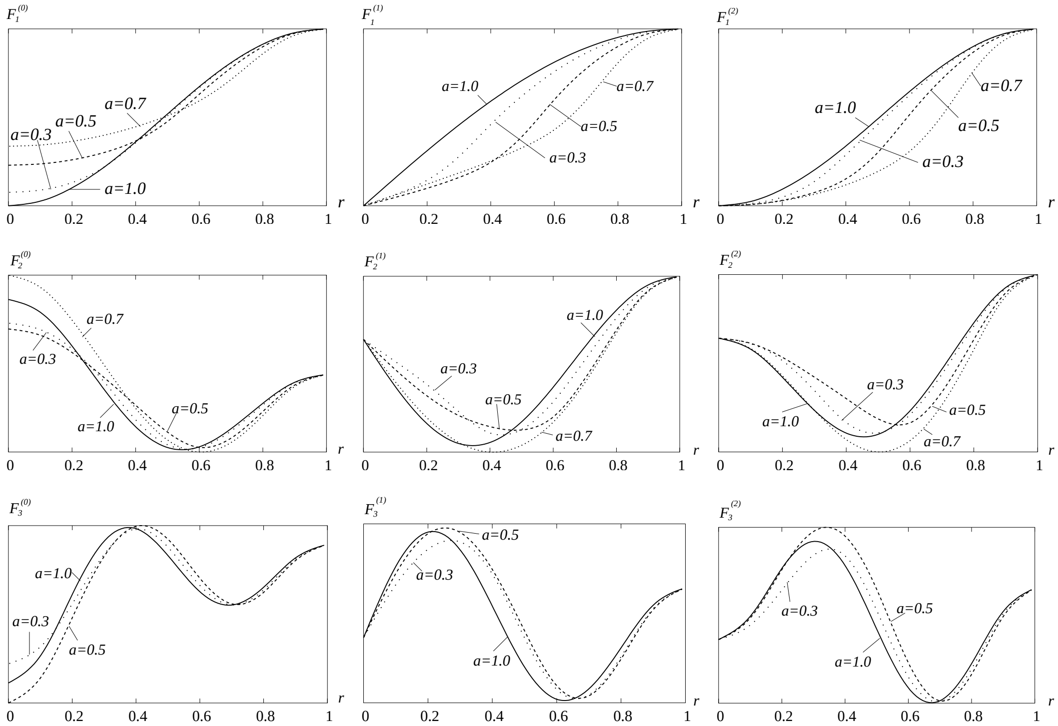

Fig. 2. Meridional profiles of the natural modes $m = 0, 1, 2;\ i = 1, 2, 3$ versus a for $h_1 = 0.1$ and $h_1 + h_2 = 1$.

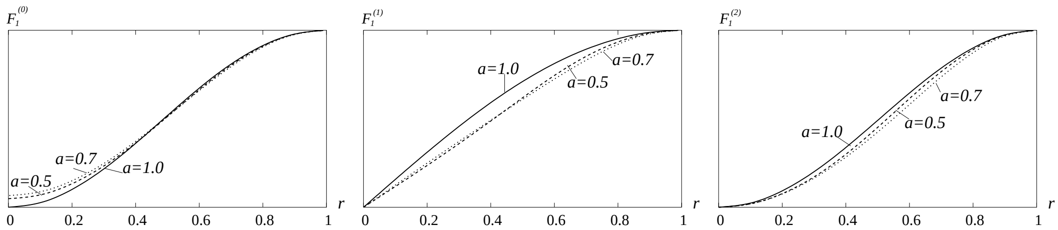

Fig. 3. The same as in Figure 2, but with $h_1 = 0.3$ (only for $F_1^{(m)},\ m = 0, 1, 2$).

$a = 0$ or 1, the natural radial surface profiles coincide with that defined for smooth circular-base tanks (there are no baffles), i.e. $F_i^{(m)}(r) = J_m(\alpha_{i,m} r),\ m = 0, 1, \ldots; i = 1, 2, \ldots$. The latter is drown with solid line. Even if h_1 is relatively small ($h_1 = 0.1$ in our examples) and $a \neq 0$ and 1, the numerical analysis establishes that $F_i(m)$ define qualitatively the same profiles as for $a = 0$. The difference is of quantitative character. Deviations of $F_i^{(m)}$ relative to $J_m(\alpha_{i,m} r)$ is larger for smaller h_1 (do compare the first rows in Figures 2 and 3). The maximum deviation depend on m and i. Numerical tests find it in the domain $0.5 < a < 0.7$.

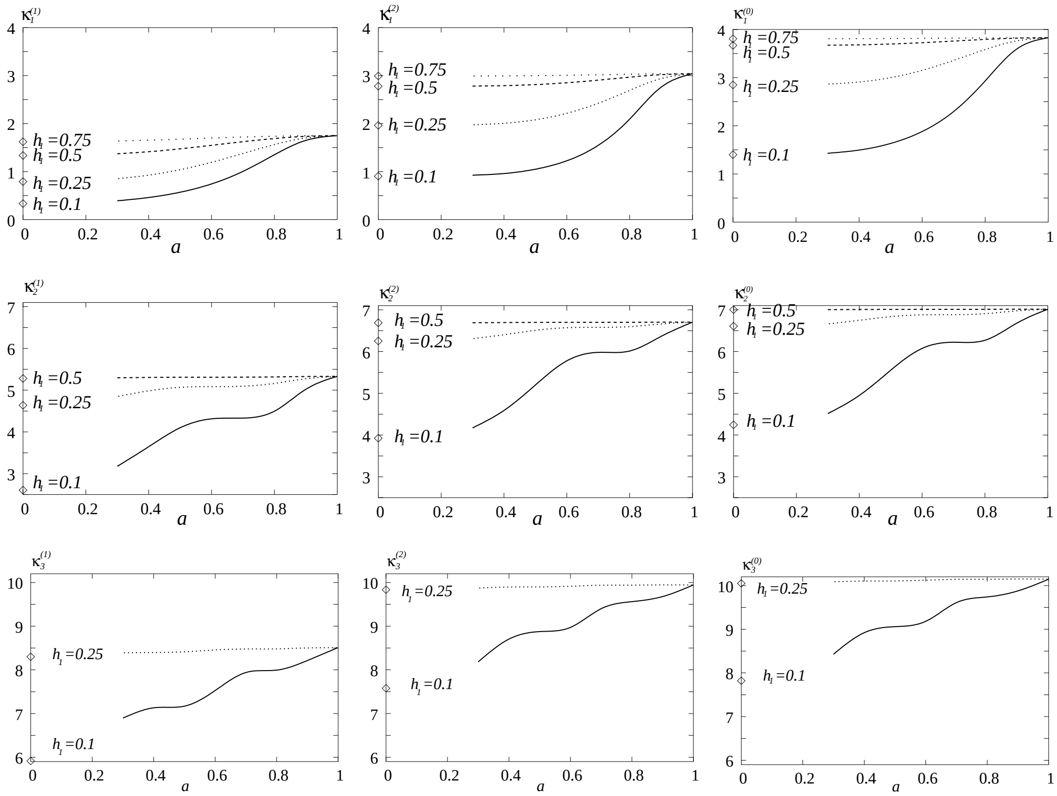

Fig. 4. Eigenvalues $\kappa_1^{(m)}$, $m = 0, 1, 2;$ $i = 1, 2, 3$ versus a for $h_1 + h_2 = 1$ and some isolated h_1.

3.3. Natural spectrum versus a

Spectral theorems by Feschenko *et al.* [22] establish monotonic evolution of $\kappa_i^{(m)}$ versus a. Besides,

$$\kappa_i^{(m)} = \begin{cases} \kappa_i^{(m)}[h], & \text{for } a = 1, \\ \kappa_i^{(m)}[h_1], & \text{for } a = 0. \end{cases}$$

This theoretical prediction is illustrated for $m = 0, 1, 2;$ $i = 1, 2, 3$ in Figure 4.

We performed numerous tests to find quantitative features of $\kappa_i^{(m)}$ versus a for different h_1 and h_2. They showed that the critical value h_1^*, so that $\kappa_i^{(m)}$ is approximately equal to $\kappa_i^{(m)}[h_1]$ for $h_1 > h_1^*$, depends on m and i. This critical value decreases with increasing i (compare first and third rows in Figure 4).

When h_1 is relatively small, the monotonic function $\kappa_i^{(m)}(a)$ has non-small gradients. Calculations showed that when $a = 0.3$, the eigenvalues $\kappa_i^{(m)}$ are close to their lower limits $\kappa[h_1]_i^{(m)}$ which are denoted on the vertical axes. This confirms the design criteria that the lowest natural frequency and mode of the baffled sloshing with $a < 0.3$ can be approximated by those for $a = 0$. The second and the third rows show also that the higher frequencies are still not close to their lower limit at $a = 0.3$, and, therefore, their influence to the nearly-shallow behaviour over the baffle and free standing wave patterns in the hole is significant. Physically, these properties imply that increasing the baffle size over $0.7R$ ($a < 0.3$) for relatively large length between the baffle plate and the free surface gives minor contribution to corresponding natural frequencies, i.e. the fluid motions under the baffle plate do not influence in this case the linear free-standing waves. However, this is not true for the higher modes (with increasing i) as shown in the last line of Figure 4. The graphs Figure 4 show also quite different quantitative behaviour of $\kappa_i^{(m)}$ versus a depending on integer parameter i, which characterises the wave steepness in radial direction of the free-standing waves. While $\kappa_i^{(m)}$ associated with the longest (in radial direction) natural waves ($i = 1$ in the first row in Figure 4) have positive second derivatives (are convex) in the range $0.3 < a < 1$, the second derivatives of $\kappa_2^{(m)}(a), \kappa_3^{(m)}(a),\ m = 0, 1, 2$ may change signs. The graphs have a shelf-like shape. Our numerical analysis shows that the ranges of small gradient coincide with the nodal points of $z = F_i^{(m)}$, while the domain of large gradients of $\kappa_i^{(m)}$ occurs nearly anti-nodal points.

3.4. Natural spectrum versus h_1

The numerical examples in Figure 5 show the monotonic dependence of $\kappa_i^{(m)}$ on $h_1 \geq 0.1$ as a quantitative numerical validation of the general spectral theory from Feschenko *et al.* [22]. Whereas $h_1 > 0.3$, the functions $\kappa_i^{(m)} = \kappa_i^{(m)}(a)$ become approximately constant, especially for the higher modes (see the second and third rows in Figure 5). An physical explanation is connected with exponential decaying of the natural modes in vertical cylindrical domains. When the baffle is situated deeper in the fluid, its influence on the standing waves around the hydrostatic plane becomes lower. Since the decaying increases with $\kappa_i^{(m)}$, the relative influence of the baffling grows with the eigenvalues. However, lowest mode associated with $\kappa_1^{(1)}$ is effected by h_1, even for relatively large h_1. The maximum influence is detected for approximately $a = 0.7$.

4. Some concluding remarks

The paper showed that the problem on linear fluid sloshing in a circular base cylindrical tank allows for semi-analytical solutions that account for analytical features of the velocity potential at the baffle edge. By adopting appropriate functional basis in a variational technique and using transmission of two boundary problems (over and under the baffle level), we obtained very robust and efficient numerical method. The method has a lot of advantages and many traditional engineering problems associated with linear fluid sloshing in a circular-base tank with a horizontal baffle can be solved. Some limitations of the method are detected with small fluid layer over the baffle and for relatively wide baffle, which covers the fluid current into the fluid volume beneath the baffle. Both cases are not of practical interest in this physical formulation, because may lead to shallow flows that are characterised by significant nonlinearities and damping.

The main advantage of the analytical approximate solutions is their applicability in non-linear modal analysis and quantification of the vorticity damping at the edges. This is subject of our forthcoming paper.

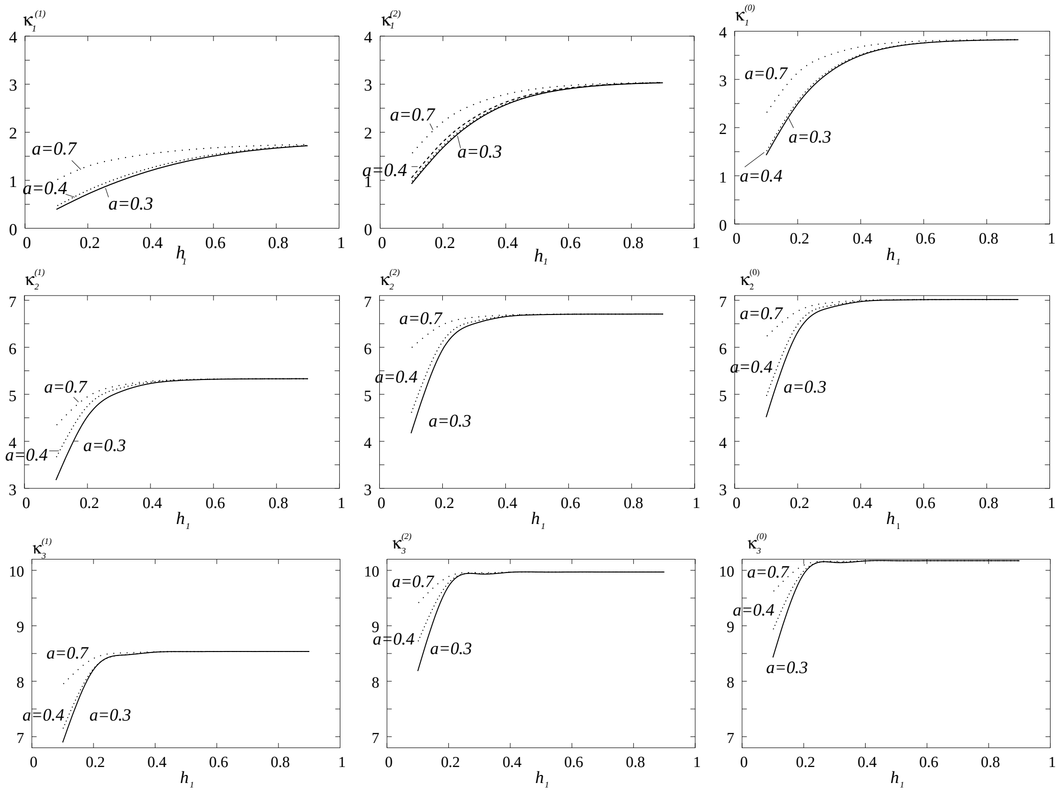

Fig. 5. Eigenvalues $\kappa_1^{(m)}$, $m = 0, 1, 2$; $i = 1, 2, 3$ versus h_1 for $a = 0.7, 0.4$ and 0.3.

References

[1] ABRAMSON, H.N.: 1969 Slosh suppression. *NASA Report SP-8031.*

[2] ARAI, M., CHENG, L.Y. & INOUE, Y.: 1992 3D numerical simulation of impact load due to liquid cargo sloshing. *J. Soc. of Nav. Arch. of Japan.* **171**, 177-185.

[3] BAUER, H.F.: 1963 Liquid sloshing in a cylindrical quarter tank. *AIAA J.* **1**, 2601-2606.

[4] BAUER, H. F.: 1964 Liquid sloshing in 45^0-compartmented sector tanks. *AIAA J.* **2**, 768-770.

[5] BAUER, H.F.: 1967 Zur Belastung, Trägheitsmoment Erhöhung und Schwappmassen Reduction durch Dämpfungsringe in Treibstofftank. *Raumfahrforschung*, **4**, 163-171.

[6] BISVAL K.S., BHATTACHARYYA S.K.& SINHA P.K.: 2003 Free-vibration Analysis of liquid-filled tank with baffles. *J. Sound and Vibration.* **259(1)** 177-192.

[7] BUZHINSKII, V.A.: 1998 Vortex damping of sloshing in tanks with baffles. *J. Appl. Maths. Mechs.* **62**, N 2, 217-224.

[8] CAMPOLO, M., SBRIZZAI, F.& SOLDATI, A.: 2003 Time-dependent flow structures and Lagrangian mixing in Rushton-impeller baffled-tank reactor. *Chemical Engineering Science*, **58**, 1615-1629.

[9] CARIOU, A.& CASELLA, G.: 1999 Liquid sloshing in ship tanks: a comparative study of numerical simulation. *Marine Structure*, **12**, 183-198.

[10] CELEBI, S.M.& AKYILDIZ, H.: 2002 Nonlinear modelling of liquid sloshing in a moving rectangular tank. *Ocean Engineering.* **29**, 1527-1553.

[11] CHESTER, W. 1968 Resonant oscillation of water waves. I. Theory. *Proc. R. Soc. of Lond.*, **308**, 5-22.

[12] CHESTER, W., BONES, J.A. 1968 Resonant oscillation of water waves. II. Experiment. *Proc. R. Soc. of Lond.*, **306**, 23-30.

[13] CHO, J.R.& LEE, H.W.: 2003 Dynamic analysis of baffled liquid-storage tanks by the structural-acoustic finite element formulation. *Journal Sound and Vibration*, **258(5)**, 847-866.

[14] CHO, J.R.& LEE, H.W.: 2004 Numerical study on liquid sloshing in baffled tank by nonlinear finite element method. *Comput. Methods Appl. Mech. Engrg.* **193**, 2581-2598.

[15] DOKUCHAEV, L.V.: 1964 On added inertia moment in a rotating cylinder with ribs. *Izvestiya AN SSSR. Mechanika i Mashinostroenie*, N 2, 168-171.

[16] EASTHAM, M.: 1962 An eigenvalue problem with parameter in boundary condition. *Quart.-Math.* **13**.

[17] ERMAKOV, V.I., MOISEYEV, G.A.& SHERSHNEV, V.G.: 1970 On perturbed motions of a body containing a cylindrical cavity with baffles. *Izvestiya AN SSSR. Mechanica tverdogo tela.* **2**, 52-61 (in Russian)

[18] FALTINSEN, O.M., ROGNEBAKKE, O.F.& TIMOKHA, A.N.: 2003 Resonant three-dimensional nonlinear sloshing in a square base basin. *Journal of Fluid Mechanics*, **487**, 1-42.

[19] FALTINSEN, O.M., ROGNEBAKKE, O.F., LUKOVSKY, I.A.& TIMOKHA, A.N.: 2000 Multidimensional modal analysis of nonlinear sloshing in a rectangular tank with finite water depth. *Journal of Fluid Mechanics*, **407**, 201–234.

[20] FALTINSEN, O.M.& TIMOKHA, A.N. 2001 Adaptive multimodal approach to nonlinear sloshing in a rectangular rank. *J. Fluid Mech.* **432**, 167-200.

[21] FALTINSEN, O.M.& TIMOKHA, A.N.: 2002 Asymptotic modal approximation of nonlinear resonant sloshing in a rectangular tank with small fluid depth. *J. Fluid Mech.* **470**, 319-357.

[22] FESCHENKO, S.F., LUKOVSKY, I.A., RABINOVICH, B.I.& DOKUCHAEV, L.V.: 1969. The methods for determining the added fluid masses in mobile cavities. *Naukova dumka, Kiev* (in Russian).

[23] GALITSIN, D.A. & TROTSENKO, V.A.: 2001 On determining the frequencies and added masses of a fluid in mobile cavities of rectangular parallelepipedal shape with partitions. *Izvestiya RAN. Mekhanica tverdogo tela.* N 2, 175-191 (in Russian).

[24] GAVRILYUK, I., LUKOVSKY, I.A.& TIMOKHA, A.N.: 2000. A multimodal approach to nonlinear sloshing in a circular cylindrical tank. *Hybrid Methods in Engineering*, **2**, N 4, 463-483.

[25] GAVRILYUK, I.P., KULIK, A.V., MAKAROV, V.L.: 2001. Integral equations of the linear sloshing in an infinite chute and their discretisation. *Computational Methods in Applied Mathematics*, **1**, 39-61.

[26] GEDIKLI, A.& ERGÜVEN, M.E.: 1999 Seismic analysis of a liquid storage tank with a baffle. *Journal of Sound and Vibration.* **223(1)**, 141-155.

[27] GEDIKLI, A.& ERGÜVEN, M.E.: 2003 Evaluation of sloshing problem by variational boundary element method. *Engineering Analysis with Boundary Elements.* N 27, 935-943.

[28] IBRAHIM, R.A., PILIPCHUK, V.N.& IKEDA, T.: 2001 Recent advances in liquid sloshing dynamics. *Applied Mechanics Research,* **54(2)**, 133-199.

[29] IKEDA, T. & NAKAGAWA, N.: 1997 Non-linear vibrations of a structure caused by water sloshing in a rectangular tank. *Journal of Sound and Vibration*, **201**, 2341.

[30] ISAACSON, M. & PREMASIRI, S.: 2001 Hydrodynamic damping due to baffles in a rectangular tank. *Canadian Journal of Civil Engineering*, **28**, 608-616.

[31] KEULEGAN, G.H. & CARPENTER, L.H.: 1958 Forces on cylinder and plates in a oscillating fluid. *J. Res. Natl. Bur. Std.* **60**, N 5, 423-440.

[32] KOZLOV, V.A., MAZ'YA, V.G., ROSSMANN, J.: 1997 Elliptic boundary value problems in domains with point singularities. *Amer. Math. Soc., Providence, RI.*

[33] KUZNETSOV, N. & MOTYGIN, O.: 2001 Sloshing problem in a half-plane covered by a dock with two gaps: monotonicity and asymptotics of eigenvalues. *C.R. Acad. Sci. Paris*, **329, Srie II b**, 791-796.

[34] LUKOVSKY, I.A., BARNYAK, M.YA.& KOMARENKO, A.N.: 1984 Approximate methods of solving the problems of the dynamics of a limited liquid volume. *Naukova dumka, Kiev.* (in Russian).

[35] LUKOVSKY, I.A.: 1990 Introduction to the nonlinear dynamics of a limited liquid volume. *Naukova Dumka, Kiev* (in Russian).

[36] MIKISHEV, G.I.: 1978 Experimental methods in the dynamics of spacecraft. Moscow:Mashinostroenie (in Russian).

[37] MIKISHEV, G.I. & CHURILOV, G.A.: 1977 Some results on experimental determining the hydrodynamic coefficients for cylinder with ribs. *In Book: "Dynamics of elastic and rigid bodies interaction with a liquid"*. Tomsk: Tomsk University, 31-37.

[38] MIKISHEV, G.I. & RABINOVICH, B.I.: 1971 Dynamics of thin-walled constructions with compartment containing a liquid. Moscow:Mashinostroenie (in Russian).

[39] MILES, J.W.: 1958 Ring damping of free surface oscillations in a circular tank. *J. Appl. Mech.* **25**, N 2, 274-276.

[40] MILES, J.W.& HENDERSON, D.M.: 1998 A note on interior vs. boundary–layer damping of surface waves in a circular cylinder. *J. Fluid Mech.* **364**, 319–323.

[41] MOAN, T.& BERGE, S.: 1997 Report of Committee I.2 "Loads". *Proceedings of 13th Int. Ship and Offshore Structures Congress*, **1**, Pergamon, 59-122.

[42] MODI, V.J., SETO, M.L. 1997 Suppression of flow-induced oscillations using sloshing liquid dampers: analysis and experiments. *J. of Wind Engineering and Industrial Aerodynamics.* **67& 68**. 611-625.

[43] MOROZOV, V.N.: 1974 Application of a finite-difference method for solving the boundary value problems of the theory of perturbed motions of a rigid body with a fluid. *In Book: "Oscillations of elastic structures with a fluid.* Novosibirsk: Electro-technical institute. 161-165 (in Russian).

[44] OCKENDON, H., OCKENDON, J.R.& WATERHOUSE, D.D. 1996 Multi-mode resonance in fluids. *J. Fluid Mech.* **315**, 317–344.

[45] RABINOVICH, B.I.: 1970 Effect of internal ribs on dynamic characteristics of a liquid in mobile containers. *Applied Math. Mech. (PMM)*, **6**, N 8, 103-111 (in Russian).

[46] SARPKAYA, T. & O'KEEFE, J.L.: 1996 Oscillating flow about two and three-dimensional bilge keels. *Journal f Offshore Mechanics and Arctic Engineering*, **118**, 1-6.

[47] SILVEIRA, M.A., STEPHENS, D.G. & LEONARD, H.W.: 1961 An experimental investigation of the damping of liquid oscillations in cylindrical tanks with various baffles. *NASA Report TN D-715.*

[48] SOLAAS, F.: 1995 Analytical and numerical studies of sloshing in tanks. *Ph.D.thesis. The Norwegian Institute of Technology. Trondheim.*

[49] TROTSENKO, V.A.: 1971 On oscillation of a liquid in a circular cylindrical tank with radial ribs. *Mathematical Physics.* Issue 9, 141-148 (in Russian).

[50] TROTSENKO, V.A.: 2003 Solutions of the boundary value problems associated with fluid dynamics in horizontal cylindrical cavities with partitions. *Nonlinear oscillations*, **6**, N 4, 401-427.

[51] WATSON, G.N.: 1922 The treatise on the theory of Bessel functions. *Cambridge University Press.*

[52] WATSON, E.B.B. & EVANS, D.V.: 1991 Resonant frequencies of a fluid container with internal bodies. *Journal of Engineering Mathematics*, **25**, 115-135.

[53] YALLA, S.: 2001 Liquid dampers for mitigation of structural response: theoretical development and experimental validation. *Ph.D. Thesis: Department of Civil Engineering and Geological Sciences Notre Dame, Indiana July 2001.*